ELSEVIER

Optical Materials 19 (2002) 275–281

OPTICAL Materials

www.elsevier.com/locate/optmat

Refractive index measurement of pure and Er^{3+}-doped ZrO_2–SiO_2 sol–gel film by using the Brewster angle technique

D. Luna-Moreno [a], E. De la Rosa-Cruz [a,*], F.J. Cuevas [a], L.E. Regalado [a], P. Salas [b], R. Rodríguez [b], V.M. Castaño [b]

[a] *Centro de Investigaciones en Optica A.C., A.P. 1-948, León, Gto. 37160, Mexico*

[b] *Departamento de Física Aplicada y Tecnología Avanzada, Instituto de Física, UNAM, A.P. 1-1010, Querétaro, Qro. 76001, Mexico*

Received 26 July 2001; accepted 29 July 2001

Abstract

The application of the Brewster angle technique and a genetic algorithm for the measurements of refractive index and thickness in tetragonal ZrO_2:Er^{3+} and ZrO_2–SiO_2 films prepared by the sol–gel process and dip–coating technique annealed at 550°C are reported. A precision higher than 99.5% and 98% in the refractive index and thickness measurements were obtained, respectively. Analysis of the capability to tune the refractive index of high-density blend films by changing the molar concentration of zirconium dioxide, with an increment rate of (0.0052 ± 0.0004)/mol, are also presented. © 2002 Elsevier Science B.V. All rights reserved.

Keywords: Sol–gel; Zirconium oxide; Brewster's angle; Refractive index measurement

1. Introduction

Zirconium dioxide is an excellent material for optical applications due to its hardness, optical transparency and high refractive index. This material has been used as an interferometric filter by coating surfaces by physical vapor deposition (PVD) [1]. Recently, the sol–gel technique has been used to produce thin films of different materials and for various applications [2]; particularly, sol–gel has been used to produce zirconium dioxide films for coating high power laser mirrors [3] and to generate passive [4] and active [5] waveguides. These films can be deposited by spinning [6] and dipping technique [7], but the last one allows coating of complex shapes and large surfaces.

Sol–gel technique is based on the hydrolysis and polycondensation of a chemical precursor of the desired material. Once the film was deposited, it was dried at low temperature obtaining a film with relatively controlled porosity by adjusting the particle size of the corresponding sol. This is extremely useful since porosity modifies the dispersing media and reduces the refractive index of the film. High-density films were obtained by subjecting the samples to different temperature cycles annealing, increasing the refractive index and

* Corresponding author. Tel.: +52-4-773-10-17; fax: +52-4-717-50-00.

E-mail address: elder@foton.cio.mx (E. De la Rosa-Cruz).

PII: S0925-3467(01)00190-2

reducing the thickness of the film. Both parameters play a key role in the performance of waveguides, the thickness can be controlled by the deposition process and the refractive index can be tuned at will from 1.46 up to 2.0 when a ZrO_2–SiO_2 blend was used. Sol–gel technique can produce a homogenous mixture of this compound. The capability to tune the refractive index opens up exciting new possibilities in the development of passive and active optical waveguides.

There are different techniques to characterize the thickness and refractive index of a waveguide, such as by measuring the transmittance [1], by ellipsometry [1] and by the Brewster angle technique [8,9]. The first one is suitable for thick films, moreover a spectrophotometer is required. Ellipsometry characterizes all optical parameters of the film but the analysis involved is complex in many practical cases. The Brewster angle technique is a simple and fast refractive index characterization method. This is suitable for any kind of transparent films and not sophisticated setup, and analysis process, is required. The aim of this work is to present the experimental results of the refractive index and thickness characterization for the blend ZrO_2–SiO_2 and $ZrO_2{:}Er^{3+}$ films prepared by dipping technique in a sol–gel solution. Also to evaluate the tuning capability of the refractive index for blend samples and the potential of the Brewster angle technique to characterize this kind of films.

2. Films preparation

Erbium-doped zirconium dioxide films were prepared as follows: 18.20 ml of zirconium propoxide (ZP) at 70 wt% solution in 1-propanol (Aldrich) was mixed with 95.20 ml of ethyl alcohol anhydrous (EA) (Baker). After 20 min of stirring, 2.45 ml of nitric acid (NA) at 69.0 vol% (Baker) and 1.0 ml of hydrochloric acid (HA) at 36.5% (Baker) were added. 2 mol% of active ions were added as a salt (erbium chloride exahydratate 99.99% of purity) and the solution was stirred for 45 min in a cool bath in order to reduce its reactivity and thus the gelation time. Three ml of CO_2-free distilled water was added dropwise and stirred vigorously for 20 min. ZrO_2–SiO_2 mixtures were prepared with different molar ratios (5, 25, 50 and 75 mol%) of ZrO_2 by using tetra-ethyl-orthosilicate (TEOS) (Aldrich) as silica precursor and, the other components, TEOS/EA/NA/HA/H_2O according to the molar composition 1/10/0.3/0.1/4. A clean BK7 substrate was used and by the dip–coating technique, sol–gel films were deposited. The immersion velocity of the substrate was 1.75 cm/min staying within the solution for 3 min. Substrate was taken up at the same velocity and annealed in an oven at 160°C for 15 min. Thicker films were obtained by repeating this process over and over again and also by increasing the viscosity of the solution. After the first thermal treatment, all samples were annealed at 160, 350 and 550°C for 15 h.

3. Brewster angle measurement

The experimental setup to measure the Brewster angle is shown in Fig. 1. A He–Ne laser centered at 632.8 nm used as a source in p polarization was directed towards a surface (substrate) coated with the probe film of refractive index n. The substrate was mounted on a rotatory stage (rotatory system θ) to scan the incident angle of the laser beam. The incident light was reflected in the interface air/film towards an optical photodetector mounted in a second rotatory stage (rotatory system 2θ) synchronized with the first rotatory system to maintain the detector-signal aligned. The intensity of

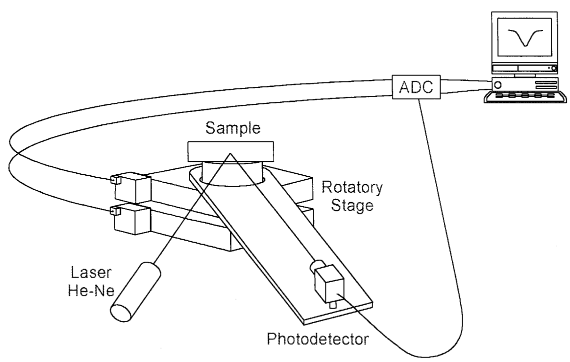

Fig. 1. Experimental setup to measure the Brewster angle. Sample and photodetector are mounted over a synchronized computer-controlled rotating system.

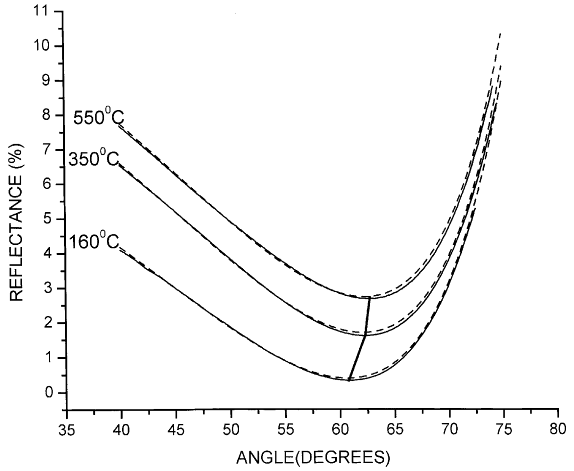

Fig. 2. Experimental results (—) and its respective fitting curve (- - -) by obtain the refractive index and thickness of the ZrO_2:Er3$^+$ film, for different temperature annealing. Curves were shifted, in the vertical, to clarify the minimum (calculated using ORIGIN™ V.6) of each one; the thick line shows the shifted of the Brewster angle according to the temperature annealing. The rms between theoretical and experimental data was 0.01.

the signal reflected was diminished as function of the incident angle, being minimum when matches the Brewster angle. The signal was recorded for a computer that also controls both rotatory systems and the experimental data for erbium-doped films annealed at 160, 350 and 550°C for 15 h are shown in Fig. 2. The corresponding results for mixed samples 5, 25, 50 and 75 mol% of zirconium dioxide annealed at 350 and 550°C are shown in Figs. 3(a) and (b), respectively. Because the experimental data were the response of the system film–substrate, and in order to obtain the refractive index and thickness of the film, the experimental data were fitted by using Fresnel's equation.

4. Theoretical fitting

The theoretical reflectance of the film was expressed by $R = \rho\rho^*$, where ρ is the amplitude reflectance calculated by the expression

$$\rho = \frac{r_{01} + r_{12}\exp[-2i\delta]}{1 + r_{01}r_{12}\exp[-2i\delta]}. \tag{1}$$

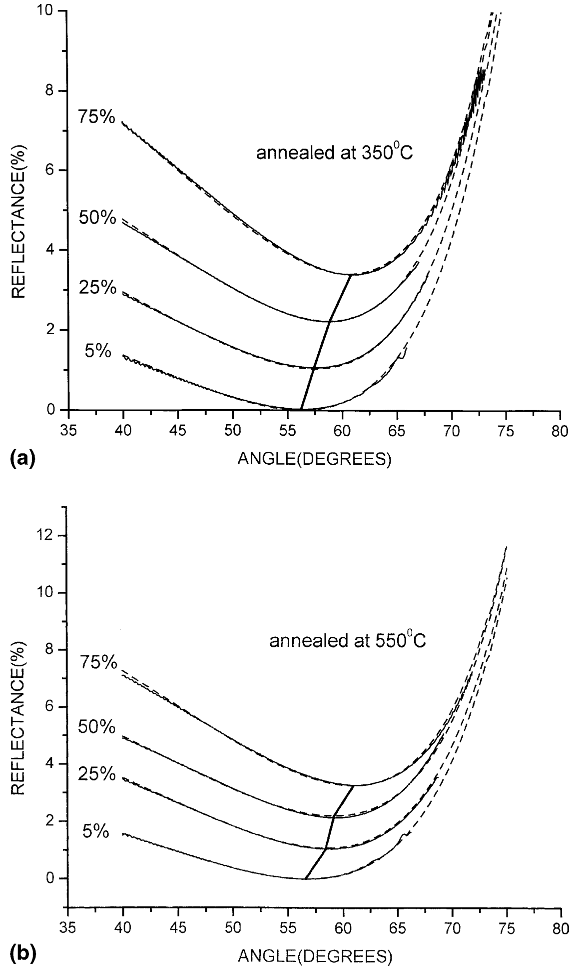

Fig. 3. Experimental results (—) for 5%, 25%, 50% and 75% of ZrO_2–SiO_2 films deposited onto a BK7 substrate, annealed for 15 h at 350°C (a) and at 550°C (b). The fitting curves (- - -) for each sample are also presented. Curves were shifted (in the vertical) to clarify the minimum of each one; the thick line shows the shifted of the Brewster angle according to molar content of ZrO_2.

Here r_{01} and r_{02} are the well-known Fresnel reflection coefficients for p polarization at the ambient medium-film and film–substrate interfaces, respectively, and the incident angle at each media are related by the Snell principle. δ is the signal phase and is expressed by the relation

$$\delta = \frac{2\pi}{\lambda}(nd\cos\theta), \tag{2}$$

where θ is the incident angle in the zirconia film, d and n are the theoretical thickness and refractive index, respectively, both were selected to match the experimental value of θ.

A genetic algorithm [10–12] was presented to carry out the refractive index and thickness calculation of thin films. The refractive index and thickness were approximated by using a non-linear function, which was selected according to the a priori knowledge of refraction and reflection principles. A population of chromosomes was codified with the parameters of the fitting function that estimates the refractive index and thickness. Then, a fitting function was modeled, which considers: (a) the experimental data and (b) the fitting function smoothness, which was selected to evaluate the chromosomes. The population of chromosomes was evolved until an established fitting average was obtained. This algorithm was used to optimize a global parametric fitting function that use a population of possible solutions, which decrease the possibility to fall in a local optimum.

The fitness function used to evaluate the population of chromosomes is given by

$$f_{\text{fitness}}(a) = \alpha - \sum_{x=1}^{N} (\text{experimental data}(x) - \rho(d,n))^2 + \lambda[(f(d,n) - f(d,n-1))^2], \quad (3)$$

where N is the experimental data size and $\rho(d,n)$ is given by Eq. (1). The second term in Eq. (3) attempts to keep the local fitting function model to the observed reflectance in least squares sense. The third term enforce the assumption of smoothness and continuity of detected non-linear reflectance. The constant α was used to convert the optimal proposal from minimization to maximization problem. The calculated reflectance was plotted in Fig. 2 for Er^{3+}-doped samples and in Figs. 3(a) and (b) for ZrO_2–SiO_2 samples annealed at 350 and 550°C, respectively. In the refractive index and thickness approximation, the following evolution parameters were used: the population size was 300 chromosomes, the crossover probability was 0.9 and the mutation probability was 0.01. The evolutive process was halted when the average fitness function got a value of 249.99 (with $\alpha = 250.0$).

5. Results and discussion

Five samples corresponding to 5, 25, 50, 75 mol% of ZrO_2 and Er^{3+}-doped zirconia film were characterized. All samples annealed at 160 and 350°C presented an amorphous structure, being tetragonal when samples were annealed at 550°C, as can be seen in Fig. 4 where the X-ray diffraction spectrum of pure ZrO_2 film is shown. This crystalline structure can be maintained up to 1000°C for blend samples, but change to monoclinic structure for erbium-doped sample. As has been shown recently, it was the presence of SiO_2 that stabilizes the tetragonal structure at 1000°C [13]. Analysis of X-ray diffraction spectra (not showed here) of the ZrO_2–SiO_2 mixtures suggested the presence of phase segregation and that the crystallite size was below 8 nm, calculated according to Scherrer's equation [14].

By using the Snell principle and the experimental Brewster angle θ_B, the refractive index n_{exp} of the system air–film–substrate was calculated using the Brewster expression $n_{exp} = \tan\theta_B$, here it was considered air as the incident medium. The value of n_{exp} represent the refractive index of the interface air–film and film–substrate, but we determined the thickness and refractive index of the film by using a fitting process with genetic algorithm and Fresnel's equations. The experimental

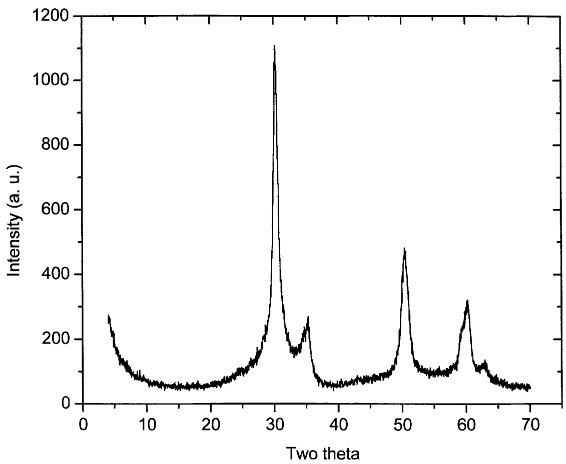

Fig. 4. X-ray spectrum for pure ZrO_2 annealed at 550°C, the main peaks are characteristic of tetragonal structure.

Table 1
(a) Experimental and theoretical results of the refractive index and thickness for ZrO_2:Er^{3+} annealed at 160, 350 and 550°C (a), for ZrO_2–SiO_2 annealed at 350°C (b) and annealed at 550°C (c)

T_a (°C)	d (nm)	$n_{exp} \pm 0.0016$	n_{theo}
(a) *For ZrO_2:Er^{3+} annealed at 160, 350 and 550°C*			
160	43.177	1.7821	1.8239
350	35.025	1.8966	1.9991
550	34.976	1.9210	2.0090
ZrO_2 (mol%)	d (nm)	$n_{exp} \pm 0.0016$	n_{theo}
(b) *For ZrO_2–SiO_2 annealed at 350°C; $T_a = 350$°C*			
5	38.600	1.5051	1.5135
25	33.200	1.5697	1.6398
50	31.400	1.6512	1.7891
75	37.900	1.8417	1.8751
(c) *For annealed at 550°C; $T_a = 550$°C*			
5	34.300	1.5166	1.5381
25	31.500	1.6318	1.7468
50	30.600	1.6775	1.8187
75	33.300	1.6775	1.9137

The rms of the fitting data was 0.01.

results of the refractive index as temperature annealing function are shown in Table 1(a) for ZrO_2:Er^{3+}, (b) and (c) for ZrO_2–SiO_2 at 350 and 550°C, respectively. Here in these tables are also shown the calculated refractive index n and thickness d of the film obtained from the fitting process. As it was expected, the refractive index increased and the thickness diminished as the temperature increased. This was the result of the organic material evaporation and a density increment by reducing the porosity of the film. Erbium-doped sample annealed at 550°C with a thickness of 35 nm presented the highest refractive index, $n = 2.009$; this was produced, in part, by the content of the active ions and also by the low content of the air volume. These values represent an increment of 10% in the refractive index and 20% of diminishment in the thickness film, with respect to the 160°C annealed sample. The calculated refractive index is little higher than recently reported by others, but present the same behavior with respect to the temperature increment [15].

Table 1(b) and (c) also shows that experimental and calculated refractive index for ZrO_2–SiO_2 samples presented an increment as function of the molar concentration of zirconium oxide. Fig. 5 shows that this behavior was linear for both samples annealed at 350 and 550°C and present an increment rate of (0.0052 ± 0.0004) and (0.0050 ± 0.0010)/mol of ZrO_2, respectively. The increment of the refractive index can be explained by the fact that silica enhances the zirconia dispersion in the solution, avoiding the zirconia aggregation and

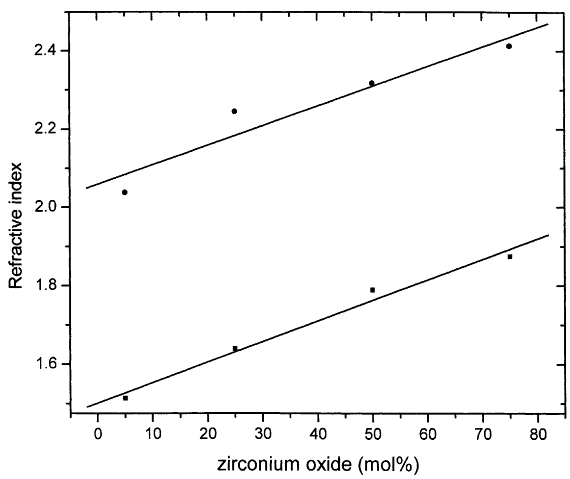

Fig. 5. Refractive index behavior as function of the molar concentration of zirconium dioxide in the blend ZrO_2–SiO_2, for samples annealed at 350°C (■) and 550°C (●); in the last case, data were shifted by 0.5 in order to clarify both curves.

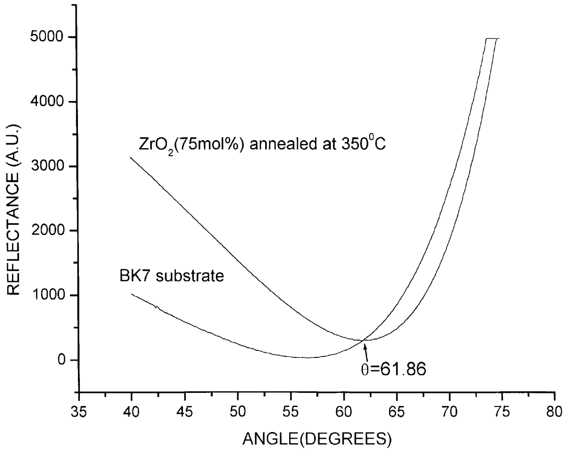

Fig. 6. Reflectance curves of the film-covered substrate and the uncoated substrate bk7 for a 75 mol% ZrO_2 film. The Brewster angle was given by the interception curves, $\theta = 61.86$, and applying Brewster's equation we obtain $n = 1.8696$ that represent an error less than 0.3% respect to the calculated with the fitting process.

thus producing small particle size and a homogenous sample.

In order to prove the confidence of our fitting process, a magnesium fluoride film was prepared by vapor deposition using a Balzer Thermical Evaporator BA510. The refractive index and thickness was measured in the deposition process with a Leybold deposition controller XTC/2 obtaining 1.3800 ± 0.0015 and 50.2 ± 0.2 nm, respectively. Theoretically, it was obtained 1.3864 and 49.4 nm, respectively; this means an error of less than 0.5% in the refractive index calculation and less than 2% in the thickness calculation. On the other hand, theoretical simulations reproduce the experimental data, demonstrating that there is no absorption effect in the film.

Another proof that we gave was the measurement of the refractive index by Abelès Brewster method [8], in this case a film-covered substrate and uncoated substrate were illuminated with p polarization light, scanning the incident angle from 40° to 75°. The interception angle of the curves corresponds to the Brewster angle of the film. This is because no light was reflected from the air-film interface at the Breswter angle of the film, then the reflectivity of the film-covered substrate is the same as that of an uncoated substrate at the Brewster angle θ_B. Thus, the refractive index of the film was calculated using the expression $n = \tan\theta_B$. Fig. 6 shows the interception of the reflectance curves for a 75 mol% of ZrO_2 film-covered substrate and the uncoated substrate. These proofs validate the fitting process in the characterization of ZrO_2 film by sol–gel process.

6. Conclusion

We have shown that it is possible to prepare high density ZrO_2:Er^{3+} and ZrO_2–SiO_2 films by the sol–gel process and the capability to tune the refractive index for blend samples. We have also shown the potential of Brewster angle method for the refractive index measurements and the potential of the genetic algorithm for the fitting process. X-ray diffraction analysis showed that tetragonal structure could be obtained at 550°C maintained up to 1000°C when SiO_2 was presented.

Acknowledgements

We acknowledge to O. Pompa and R. Mendoza for their help in the preparation of magnesium fluoride film and figures of the present work, respectively.

References

[1] H.A. Mcleod, in: Thin Film Optical Filters, second ed., Adam Hilger, Bristol, 1986, p. 519.
[2] H. Floch, P. Belleville, International Symposium on Optical Interference Coating, Grenoble, France, 1994.
[3] I.M. Thomas, SPIE 2288 (1994) 50.
[4] R. Brenier, C. Urlacher, J. Mugnier, M. Brunel, Thin Solid Films 338 (1999) 136.
[5] M. Zevin, R. Reisfeld, Opt. Mater. 8 (1997) 37.
[6] M.C. Matos, A.R. Carvalho, R.M. Almeida, SPIE 1758 (1992) 77.
[7] B.E. Yoldas, SPIE 1328 (1990) 296.
[8] G. Hass, R.E. Thun, Precision measurement in thin film optics, in: H.E. Bennet, J.M. Bennet (Eds.), Physics of Thin Films, vol. 4, Academic Press, New York, 1967 (Chapter 1).
[9] O.S. Heavens, H.M. Liddell, Appl. Opt. 4 (5) (1965) 629.

[10] M. Mitchel, An Introduction to Genetic Algorithms, MIT Press, London, 1998.
[11] D.E. Goldberg, Genetic Algorithms in Search, Optimization, and Machine Learning, Addison-Wesley, Reading, MA, 1989.
[12] F. Man, K.S. Tang, S. Kwong, Genetic Algorithms, Springer, Berlin, 1999.
[13] P. Salas, E. De la Rosa-Cruz, D. Mendoza-Anaya, P. González-Martínez, V.M. Castaño, R. Rodríguez, Mater. Res. Innovat. 64 (2000) 4.
[14] B.D. Cullity, in: Elements of X-ray Diffraction, second ed., Addison-Wesley, Reading, MA, 1978, p. 102.
[15] C. Urlacher, C. Marco de Luca, E. Bernstein, B. Jacquier, J. Mugnier, Opt. Mater. 12 (1999) 19.